Mathematical Geology, Vol. 30, No. 1, 1998

Interpolation with Splines in Tension: A Green's Function Approach[1]

Paul Wessel[2] and David Bercovici[2]

Interpolation and gridding of data are procedures in the physical sciences and are accomplished typically using an averaging or finite difference scheme on an equidistant grid. Cubic splines are popular because of their smooth appearances; however, these functions can have undesirable oscillations between data points. Adding tension to the spline overcomes this deficiency. Here, we derive a technique for interpolation and gridding in one, two, and three dimensions using Green's functions for splines in tension and examine some of the properties of these functions. For moderate amounts of data, the Green's function technique is superior to conventional finite-difference methods because (1) both data values and directional gradients can be used to constrain the model surface, (2) noise can be suppressed easily by seeking a least-squares fit rather than exact interpolation, and (3) the model can be evaluated at arbitrary locations rather than only on a rectangular grid. We also show that the inclusion of tension greatly improves the stability of the method relative to gridding without tension. Moreover, the one-dimensional situation can be extended easily to handle parametric curve fitting in the plane and in space. Finally, we demonstrate the new method on both synthetic and real data and discuss the merits and drawbacks of the Green's function technique.

KEY WORDS: gridding, interpolation, splines.

INTRODUCTION

In the physical sciences, and in the earth sciences in particular, data may be resampled onto an equidistant grid or to arbitrary locations or times. Numerous methods have been proposed to facilitate this task, including simple weighted-average operators (e.g., Wegman and Wright, 1983), statistical approaches such as kriging (Clark, 1979; Olea, 1974), two-dimensional splines (Briggs, 1974; Inoue, 1986; Sandwell, 1987; Smith and Wessel, 1990; Swain, 1976), and projections onto convex sets (POCS) (Menke, 1991). Because of their smoothness, splines have become one of the most popular methods used for gridding.

[1]Received 4 October 1996; revised 2 April 1997.

[2]Department of Geology & Geophysics, School of Ocean and Earth Science and Technology, University of Hawaii at Manoa, 1680 East-West Road, Honolulu, Hawaii 96822. e-mail: wessel@soest.hawaii.edu.

0882-8121/98/0100-0077$15.00/1

Swain (1976), implementing the approach suggested by Briggs (1974), designed a FORTRAN program for minimum curvature spline interpolation that has been used widely in the earth-science community. This method produces a gridded surface that minimizes the squared curvature integrated over the entire surface; it yields the smoothest possible surface which can match the given data constraints. One criticism of the minimum curvature method is its tendency to introduce extraneous inflection points (Schweikert, 1966); to minimize curvature, the curve (or surface) actually may contain large oscillations between data constraints. This undesired behavior can be suppressed by imposing tension on the curve (or surface). Smith and Wessel (1990) presented a gridding algorithm which used continuous curvature splines in tension. A computer program using their algorithm is distributed with the Generic Mapping Tools (GMT) software package (Wessel and Smith, 1991; Wessel and Smith, 1995) and now is widely used.

Most of the gridding methods discussed here require a numerical solution on a uniform grid. In particular, both the methods of Swain (1976) and Smith and Wessel (1990) involve the solution to partial differential equations using finite-differences techniques. Sandwell (1987) presented a new method for minimum curvature gridding based on the Green's function of the biharmonic operator. In his method, the interpolating surface is a linear combination of Green's functions centered at each data constraint; the relative strengths of these components are determined by solving a square linear system of equations. Using Green's functions has both advantages and disadvantages. As Sandwell (1987) reports, the improvements over the conventional methods include (1) enhanced flexibility because both data values and gradients can be used to constrain the surface, (2) by setting the smallest eigenvalues of the linear system to zero a least-squares fit to noisy data can be obtained, and (3) no uniform grid is required, hence the surface can be constructed at arbitrarily spaced locations. However, numerical instabilities can occur when the ratio of the maximum point separation to the minimum point separation is large. Furthermore, computer time is proportional approximately to the cube of the number of data constraints, making the method slow for situations with dense data coverage. In addition, being a minimum curvature technique it suffers from the same tendency to develop extraneous inflection points mentioned earlier.

In this paper, we will generalize the technique of Sandwell (1987) to include tension. First, we will derive the Green's functions and their gradients for the one-, two-, and three-dimensional spline in tension and discuss their properties. We then will test the new method on both data values and gradients, and discuss to what extent the inclusion of tension may remedy some of the shortcomings of Sandwell's (1987) minimum curvature method. Our techniques have been implemented in the Matlab language; source code and example data are available through the World Wide Web at URL http://www.soest.hawaii.edu/wessel/wes-

sel.html. Mitásová and Mitás (1993) also have discussed recently interpolation using a regularized spline with tension. Our presentation differs from theirs in that we formulate the interpolation problem for data in 1, 2, and 3 dimensions, including spatial curve fitting, and we discuss the stability of the solutions and the effect of tension in terms of the eigenvalue spectrum. We also allow for an approximate fit rather than exact interpolation which may be inappropriate for noisy datasets.

METHOD

Spline interpolation, whether in one or two dimensions, physically corresponds to forcing a thin elastic beam or plate to pass through the data constraints. Away from the data points the curve (or surface) will take on the shape that minimizes the strain energy (Timoshenko and Woinowsky-Krieger, 1959). This shape will depend on the amount of tension being exerted as well as the stiffness of the material. Although perhaps less physically intuitive, the same interpolation principle can be applied in three dimensions.

The point-force Green function $\phi(\mathbf{x})$ for a spline in tension must satisfy

$$D\nabla^4\phi(\mathbf{x}) - T\nabla^2\phi(\mathbf{x}) = \delta(\mathbf{x}) \tag{1}$$

Here, ∇^4 and ∇^2 are the biharmonic and Laplace operators, respectively, D is the flexural rigidity of the plate, T the tension applied at the boundaries, and $\mathbf{x}$ the position vector. Following Sandwell (1987), the general situation of N data constraints w_j at locations $\mathbf{x}_j$ results in the equation

$$D\nabla^4 w(\mathbf{x}) - T\nabla^2 w(\mathbf{x}) = \sum_{j=1}^{N} c_j \delta(\mathbf{x} - \mathbf{x}_j) \tag{2}$$

with solution

$$w(\mathbf{x}) = \sum_{j=1}^{N} c_j \phi(\mathbf{x} - \mathbf{x}_j) \tag{3}$$

The coefficients c_j are determined by evaluating (3) at each data constraint and solving the square linear system that results:

$$w_i = \sum_{j=1}^{N} c_j \phi(\mathbf{x}_i - \mathbf{x}_j) \qquad i = 1, N \tag{4}$$

or in matrix form

$$\mathbf{G} \cdot \mathbf{c} = \mathbf{w} \tag{5}$$

where $\mathbf{G}$ is the Green's matrix or data kernel. If the data constraints in fact are gradient values, the slopes s_i in the directions $\mathbf{n}_i$ are used in solving the linear

system

$$s_i = (\nabla w \cdot \mathbf{n})_i = \sum_{j=1}^{N} c_j \nabla\phi(\mathbf{x}_i - \mathbf{x}_j) \cdot \mathbf{n}_i \qquad i = 1, N \tag{6}$$

In mixed situations where N_0 data points and N_1 slopes constrain the interpolation (4) is used to evaluate the first N_0 equations and (6) to evaluate the last N_1 equations in the total $(N_0 + N_1)$ by $(N_0 + N_1)$ square linear system. Once $\mathbf{c}$ has been determined, the complete solution $w(\mathbf{x})$ is evaluated using (3).

We solve (1) by first introducing the new variable

$$\psi(\mathbf{x}) = \nabla^2\phi(\mathbf{x}) \tag{7}$$

$\psi(\mathbf{x})$ is the curvature of the Green's function. Substituting (7) into (1) gives

$$D\nabla^2\psi(\mathbf{x}) - T\psi(\mathbf{x}) = \delta(\mathbf{x}) \tag{8}$$

We take the Fourier transform to obtain

$$-k^2 D\Psi(\mathbf{k}) - T\Psi(\mathbf{k}) = 1 \tag{9}$$

where $\mathbf{k}$ is the wavenumber vector, $k^2 = \mathbf{k} \cdot \mathbf{k}$, and $\Psi(\mathbf{k})$ is the Fourier transform of $\psi(\mathbf{x})$. In the wavenumber domain the solution becomes

$$\Psi(\mathbf{k}) = -\frac{1}{D}\left(\frac{1}{k^2 + p^2}\right) \tag{10}$$

Here we have introduced

$$p^2 = T/D \tag{11}$$

So far, equation (10) applies for spaces of any dimension. However, the solutions for $\psi(\mathbf{x})$ and ultimately $\phi(\mathbf{x})$ are specific to each dimension; we will proceed to solve them separately for 1-D, 2-D, and 3-D. For higher dimensions, the Green's functions are singular at the origin and cannot be used for spline interpolation. The delta-function in (1) implies that the Green's function must be symmetric about the origin of the delta function; in addition we require that $\phi(\mathbf{x})$ and its first derivative be zero for $\mathbf{x} = \mathbf{0}$. Apart from the differences in the resulting Green's functions and their gradients, the solutions to the interpolation problems in all dimensions are obtained in exactly the same manner via (3)–(4).

1-D Interpolation with Splines in Tension

Interpolation in one dimension using splines in tension has been proposed by Schweikert (1966) and implemented by Cline (1974). However, the implementations of such algorithms are tedious and error-prone. The Green's function

approach suggested by Sandwell (1987) for the 1-D cubic spine applies also to splines in tension. Starting from (10), where $k = |\mathbf{k}|$ now is the linear wavenumber, we take the inverse 1-D Fourier transform and obtain

$$\psi(x) = -\frac{1}{D}\int_{-\infty}^{\infty}\frac{e^{ikx}dk}{k^2 + p^2} = -\frac{1}{D}\frac{\sqrt{\pi/2}}{p}e^{-p|x|} = \frac{A}{p}e^{-p|x|} \tag{12}$$

Integrating twice and imposing symmetry gives

$$\phi(x) = \frac{A}{p^3}e^{-p|x|} + B|x| + C \tag{13}$$

The gradient of the Green's function must be continuous at the origin. Imposing continuity of $\phi'(x)$ gives $B = A/p^2$; requiring $\phi(0) = 0$ gives $C = -A/p^3$. After ignoring the overall scale factor A/p^3 (which becomes incorporated into $\mathbf{c}$) we obtain the Green's function for a 1-D spline in tension:

$$\phi(x) = e^{-p|x|} + p|x| - 1 \tag{14}$$

with its gradient

$$\frac{d\phi(x)}{dx} = p(1 - e^{-p|x|})\frac{x}{|x|} \tag{15}$$

As $p \to 0$ the solutions (14)–(15) behave similar to the functions $|x|^3$ and $|x|$ as determined by Sandwell (1987) for the special situation $T = 0$, but they are not valid for $p = 0$.

The functions (14–15) also can be used for parametric curve fitting in the plane or in space. Following Cline (1974) we introduce simply a distance variable

$$d_i = \begin{cases} 0, & i = 1 \\ d_{i-1} + |\mathbf{x}_i - \mathbf{x}_{i-1}|, & i = 2, N \end{cases} \tag{16}$$

and determine the two (or three) interpolations $\mathbf{x}(d)$ for each separate coordinate in $\mathbf{x}$ (e.g., for a spatial parametric curve $\mathbf{x}(d) = [x(d), y(d), z(d)]$) with d the independent variable, that is, the Green's matrix $\mathbf{G}$ is calculated once using the d_i and we determine two (or three) sets of amplitudes by solving the augmented matrix equation

$$[\mathbf{c}_x \quad \mathbf{c}_y \quad \mathbf{c}_z] = \mathbf{G}^{-1}[\mathbf{x} \quad \mathbf{y} \quad \mathbf{z}] \tag{17}$$

Here, $\mathbf{x}$, $\mathbf{y}$, and $\mathbf{z}$ are the observed coordinates (i.e., data constraints) for the desired spatial curve ($\mathbf{c}_z$ and $\mathbf{z}$ are neglected for curves in the plane). The interpolated values $\mathbf{x}(d)$ thus are determined via (3) for each component, pre-

sumably for a monotonically increasing (or decreasing) range of d values that include the values calculated in (16).

2-D Interpolation with Splines in Tension

Before we attempt to solve (1) let us consider first the two end-member situations $T = 0$ and $D = 0$. $T = 0$ is the situation studied by Sandwell (1987). It is well known that the Green's function in this example becomes (Greenberg, 1971; Sandwell, 1987)

$$\phi(\mathbf{x}) = |\mathbf{x}|^2 \log(|\mathbf{x}|) \tag{18}$$

On the other hand, letting $D \rightarrow 0$ indicates we are interpolating using an elastic membrane with no internal rigidity; the corresponding Green function is

$$\phi(\mathbf{x}) = \log(|\mathbf{x}|) \tag{19}$$

which is singular at the origin and not suitable for gridding. However, we anticipate that the general solution to (1) in 2-D will retain the characteristics of (18) and (19) as D and T approach their extreme values. Because of axisymmetry we transform (10) back to the space domain using the inverse Hankel transform:

$$\psi(\mathbf{x}) = -\frac{1}{D}\int_0^\infty \frac{J_0(kr)kdk}{k^2 + p^2} = -\frac{1}{D} K_0(p|\mathbf{x}|) = AK_0(p|\mathbf{x}|) \tag{20}$$

where $k = |\mathbf{k}|$ becomes the radial wavenumber and K_0 is the modified Bessel function of the second kind and order zero. Substituting (20) into (7) gives (with $r = |\mathbf{x}|$)

$$\frac{1}{r}\frac{d}{dr}\left(r\frac{d\phi}{dr}\right) = AK_0(p|\mathbf{x}|) \tag{21}$$

Integrating twice results in

$$\phi(\mathbf{x}) = \frac{A}{p^2} K_0(p|\mathbf{x}|) + B\log|\mathbf{x}| + C \tag{22}$$

Realizing that $K_0(\mathbf{x}) \sim -\log(x)$ for small x we must select $B = A/p^2$ such that no singularity occurs at the origin. C is determined from the condition $\phi(0) = 0$; we determine $C = A\log(p)/p^2$ and discard the common factor A/p^2 to give the final Green's function as

$$\phi(\mathbf{x}) = K_0(p|\mathbf{x}|) + \log(p|\mathbf{x}|) \tag{23}$$

where the gradient of the Green's function is

$$\nabla\phi(\mathbf{x}) = p\left[\frac{1}{p|\mathbf{x}|} - K_1(p|\mathbf{x}|)\right]\frac{\mathbf{x}}{|\mathbf{x}|} \tag{24}$$

Let us examine the characteristics of the Green's function for 2-D splines in tension more closely. When $T \to 0$ the parameter $p \to 0$ as well, hence the arguments to ϕ will be small. For small arguments the leading terms in K_0 is (Abramowitz and Stegun, 1970)

$$K_0(x) \sim -\log x(1 + \alpha x^2 + \ldots) \tag{25}$$

which implies that

$$\phi(x) \sim x^2 \log x \tag{26}$$

Therefore, for low tension our solution is expected to approach the minimum curvature solution (18) of Sandwell (1987). Note, however that our expression is only valid for $p > 0$ because of the p^{-2} factor in (22); for $p = 0$ we must use (18) instead.

As T increases so does p, and the arguments to ϕ will be large. Because $K_0(x) \sim e^{-x}$ for large x it is clear that $\phi(x) \sim \log x$. Thus, we anticipate a surface dominated by tension. Note, however, that $\phi(x)$ does not develop a singularity as is the limiting situation of $D = 0$ [i.e., Eq. (19)]. Figure 1 displays normalized examples of ϕ and $\nabla\phi$ (in the radial direction) for various values of tension. The trade-off between $\log(p|x|)$ and $K_0(p|x|)$ produces a continuous spectrum of Green's functions; as $p \to 0$ we approach the biharmonic Green's function, $x^2 \log x$.

From this discussion it is clear that $\phi(x)$ is sensitive to the selection of units. In fact, p has units such that the product $p|\mathbf{x}|$ becomes nondimensional. Scaling all distances by a constant factor is equivalent to multiplying the parameter p by the same amount. Thus, unlike (18), (23) is scale-sensitive and we must normalize our horizontal dimensions in order for p to have the same meaning for different datasets. In practice we know that by multiplying distances by $\alpha = 50/r_{\max}$ where $r_{\max}$ is the greatest point separation, and introducing the nondimensional parameter τ to represent the portion of the strain energy resulting from tension relative to the total strain energy (i.e., normalized $p^2 = \tau/(1 - \tau)$), the Green's function exhibits its full range of behavior on the interval $0 < \tau < 1$ because $p \to \infty$ as $\tau \to 1$. Note that in the finite difference implementation of Smith and Wessel (1990) the distances are normalized implicitly by the prescribed grid spacing; hence selecting $\tau = 0.3$ will give different results depending in the selected grid spacing.

3-D Interpolation with Splines in Tension

For $T = 0$, the spline interpolation in three dimensions corresponds to multiquadric interpolation (Hardy, 1971; Hardy and Nelson, 1986; Sandwell,

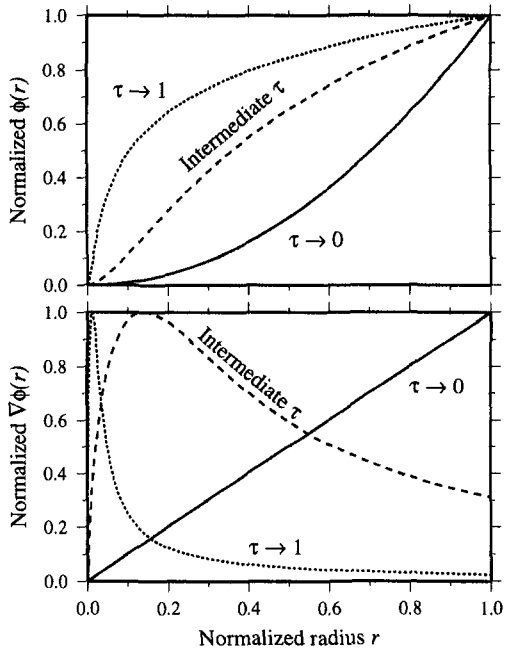

Figure 1. (Top panel) Radial cross section of Green's function $\phi(r)$ for two-dimensional spline in tension. For no tension solution approaches $-r^2 \log(r)$, whereas for high tension $\phi(r)$ takes on a $\log(r)$ shape without singularity origin. (Bottom panel) Radial cross section of gradient $\nabla\phi(r)$ in radial direction for various values of tension. Note that as $\tau \rightarrow 1$ (with τ defined as $p^2 = \tau/(1 - \tau)$) solution remains finite at origin. All values have been normalized to fit on same diagram.

1987). We pursue the solution for the general situation by taking the 3-D inverse Fourier transform of (10) for spherical symmetry (Bracewell, 1978):

$$\psi(|\mathbf{x}|) = -\frac{1}{D}\int_0^\infty \frac{\text{sinc}(k|\mathbf{x}|)k^2\,dk}{(k^2 + p^2)} = -\frac{\pi}{2D}\frac{1}{|\mathbf{x}|}e^{-p|\mathbf{x}|} \tag{27}$$

In this example, $k = |\mathbf{k}|$ is the spherical wavenumber. Substituting (27) into (7) yields

$$\frac{1}{r^2}\frac{d}{dr}\left(r^2\frac{d\phi}{dr}\right) = -\frac{\pi}{2D}\frac{1}{|\mathbf{x}|}e^{-p|\mathbf{x}|} = A\frac{1}{|\mathbf{x}|}e^{-p|\mathbf{x}|} \tag{28}$$

where $r = |\mathbf{x}|$. Again, integrating twice gives

$$\phi(\mathbf{x}) = \frac{A}{p^2|\mathbf{x}|} e^{-p|\mathbf{x}|} + \frac{B}{|\mathbf{x}|} + C \tag{29}$$

As before, the conditions on ϕ and $d\phi/dr$ at the origin require $B = -A/p^2$ and $C = A/p$. Ignoring the common factor A/p we obtain the final Green's function for 3-D spline in tension interpolation as

$$\phi(\mathbf{x}) = \frac{1}{p|x|} (e^{-p|\mathbf{x}|} - 1) + 1 \tag{30}$$

with its gradient being

$$\nabla\phi(\mathbf{x}) = \frac{1}{p|\mathbf{x}|^2} [1 - e^{-p|\mathbf{x}|}(p|\mathbf{x}| + 1)] \frac{\mathbf{x}}{|\mathbf{x}|} \tag{31}$$

As $p \to 0$ (except $p = 0$) we see that $\phi(\mathbf{x}) \to |\mathbf{x}|$ which is the solution obtained by Sandwell (1987). We now will explore the use of the Green's functions for both synthetic and real data in following section.

EXAMPLES

Our first example demonstrates splines in tension for both 1-D data, planar curves, and spatial curves and illustrates the effect of tension on the unwanted oscillations associated with the standard cubic spline solution. Figure 2A reproduces the 1-D spline example used by Sandwell (1987). The heavy solid line is the standard cubic spline ($\tau = 0$) with unconstrained end conditions. Adding tension ($\tau = 0.8$; thin solid line) reduces the ringing, whereas ignoring the smallest eigenvalues produces a least-squares fit (dotted line). By letting $\tau \to 1$ we can eliminate completely the wild oscillations about $x = 5$. The limiting situation $\tau = 1$ corresponds to linear interpolation. In Figure 2B we demonstrate curve fitting in the plane on a small subset of points making up the coastline of Long Island, NY in the GSHHS database (Wessel and Smith, 1996). A linear interpolation between these points would produce an unrealistic coastline. Using a spline can improve the appearance of the coastline, but the oscillatory nature of the cubic spline can create intermediate points leading to crossovers between coast line segments (dotted line). A spline in tension ($\tau = 0.95$; solid line) produces a relatively smooth curve without crossovers. Relaxing the requirement of exact interpolation (dashed curve) can remove some of the short-wavelength noise introduced by the digitizing process but is not guaranteed to yield an interpolation free of crossovers. Finally, in Figure 2C we have made a synthetic 3-D dataset from the parametric curve $x(s) = (s^{3/2} + \pi) \cdot \cos(s)$, $y(s) = (s^{3/2}$

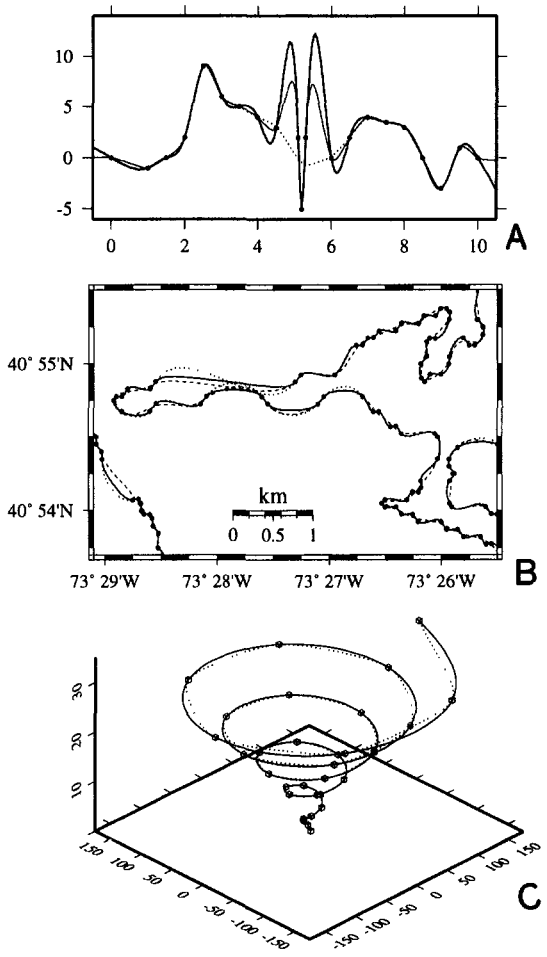

Figure 2. A, 1-D interpolation with splines in tension using synthetic data of Sandwell (1987). Heavy solid line is spline with no tension and unconstrained endpoints. Thin solid line has $\tau = 0.8$ and moderately reduces ringing. Finally, dotted line represents least-squares fit in which some small eigenvalues have been zeroed out. B, Coastline data for northern Long Island, NY. Interpolation with planar-valued cubic spline yields crossovers (dotted curve). Heavy tension ($\tau = 0.95$; solid curve) remedies problem. Least-squares fit (dashed curve) reduces short-wavelength digitizing noise in original data. C, Vector-valued parametric curve interpolated from synthetic data points approximating expanding helix. Cubic spline curve (solid curve) is in this example better able to reproduce smoothness of original data; tension introduces noticeable kinks at data constraints.

$+ \pi) \cdot \sin(s)$, $z(s) = s$ on the interval $s = [0, 10\pi]$ sampled every $\pi/3$. We then interpolated these (x_i, y_i, z_i) points using no tension (solid curve) and with tension ($\tau = 0.75$; dotted curve). In this particular example where the data constraints were sampled from a smooth curve, the $\tau = 0$ solution gives a more pleasing result than the solution with tension. Although only used for the 1-D situation (Fig. 2A), slope constraints can be implemented for parametric curve fitting as well.

Our next examples explore the use of (23) and (24) for gridding of 2-D data. We will first examine the effect of tension on 2-D surfaces. The circles in Figure 3 represent the locations of our data constraints; they all have $z_i = 0$ except the point at the origin which has $z_i = 1$. The heavy solid line is the minimum curvature solution ($\tau = 0$) along a radial section, exhibiting the typical fluctuations between data constraints. Moderate tension ($\tau = 0.4$; dotted line) significantly reduces the ringing, whereas strong tension ($\tau = 0.9$; dashed line) completely eliminates it. In all situations the solution exactly interpolates the data.

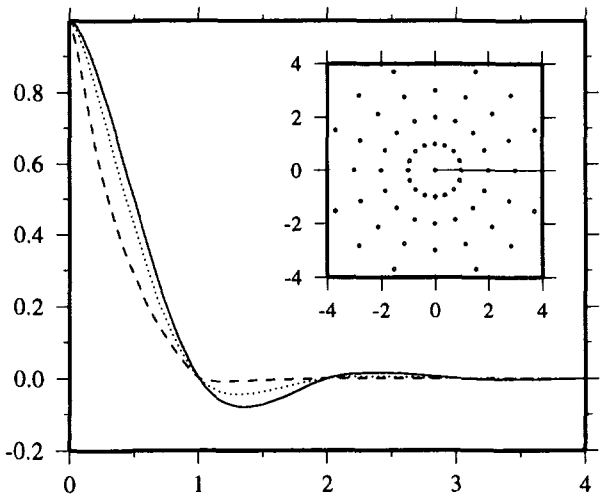

Figure 3. Radial cross section of 2-D interpolation with axisymmetrical data constraints (shown in inset) where all data values equal zero except point at origin which is unity. Heavy solid line represents minimum curvature solution ($\tau = 0$) exhibiting ubiquitous ringing. Intermediate dotted line shows reduced ringing for $\tau = 0.4$, whereas heavy tension (dashed line; $\tau = 0.9$) completely suppress extraneous inflection points.

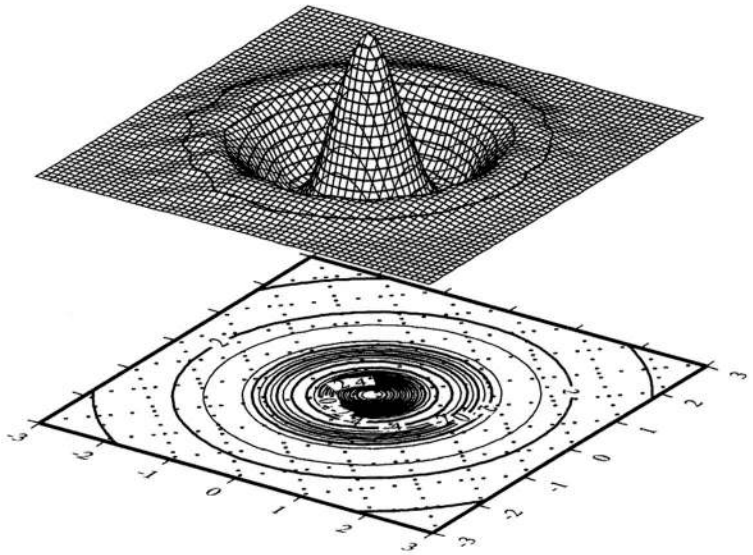

Figure 4. Damped cosine surface reconstructed from samples of directional gradients taken along two sets of crossing tracks (indicated below). Single data constraint was added to slope constraints in order to fix absolute level of surface.

One advantage of the Green function method is the ease with which slope constraints can be incorporated into the solution. Figure 4 (bottom section) shows a contour map of the surface $z = 10 \exp(-r^2/2) \cos(\pi r) + 2$. We sampled the slopes of this dataset along a set of crossing tracks (small solid circles) and solved for the relative amplitudes using (17). When only slope data are used the mean value of the resulting surface is not recovered. Therefore, we added one additional data constraint ($z_i = 12$ at the origin); using $\tau = 0.25$ we recovered the surface displayed in Figure 4 (top section).

Our final 2-D example shows the result of gridding multibeam bathymetry off the island of Hawaii. Figure 5 displays the 25-meter contours within the areas of the map that have data constraints. We used a tension factor of 0.5. The bathymetry data were preprocessed by determining the average bathymetry within each 1×1 arc second grid box; this reduced the number of data points to $N = 1755$. The resulting N by N matrix equation then was solved for the amplitudes **c**. Because no grid is necessary when evaluating the surface we only used (3) within the areas constrained by data. This is in contrast to finite-difference techniques which require us to propagate the solution across all the unconstrained nodes.

Our last example demonstrates the use of (30) for interpolating points in

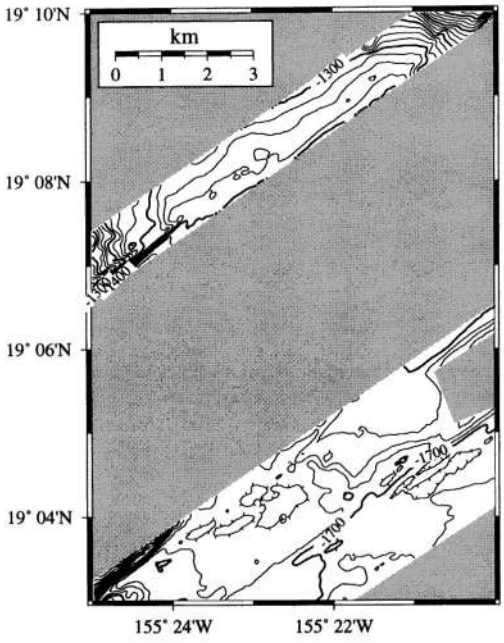

Figure 5. Spline-in-tension gridding of multibeam bathymetry off island of Hawaii. Gray areas have no data; remaining areas have dense, uniform data coverage. Because Green's function method does not require grid, we only evaluated solution at output points where data existed. Contour interval is 25 m.

3-D. We used this Green's function to grid the uranium oxide content (in %) of a carnonite body in Jurassic sediments in the Colorado Plateau (table 5.23 in Davis, 1986). This dataset was interpolated with $\tau = 0.1$ onto an equidistant (x, y, z) grid and the 10% contour for each horizontal slice was determined (Fig. 6). The resulting plot shows a surface of constant (10%) value which outlines the region of high uranium oxide concentration in this rock formation.

DISCUSSION

One disadvantage of the Green's function technique is the possibility that the matrix in (5) becomes singular. Sandwell (1987), using single precision computations, determined that 1-D interpolation became unstable when more than about 40 irregularly spaced points were used, thus rendering the method almost useless. For 2-D gridding the situation improved somewhat in that linear

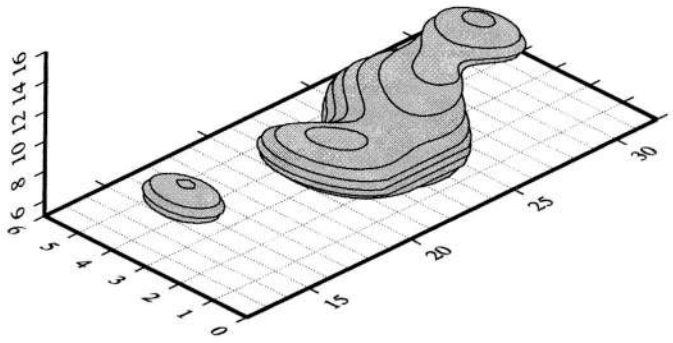

Figure 6. Example of interpolation with splines in tension for 3-D dataset. Sparsely sampled uranium oxide concentrations were interpolated evenly using (30) and 10% contour determined from contours of data slices. Tension of 0.1 was used.

systems as large as 400 × 400 could be solved (Sandwell, 1987). We determined that using double precision calculations dramatically improved the usefulness of the method. Using implementations of our methods in Matlab, we directly solved gridding problems involving more than 5000 data constraints, resulting in a 5000 × 5000 linear system without any problems of instability. However, because the memory requirements go as N^2 the method generally is not practical for situations with large amounts of data constraints. In such situations a finite difference approach will be more economical. Alternatively, one can split the data region into subset which can be gridded individually and blended together into a final grid (Mitśová and Mitás, 1993; Sandwell, 1987). On the other hand, when the number of data constraints are moderate and the grid size is large our method is fast because evaluating (3) at the grid nodes is less computer-intensive than solving the finite difference equations by iterations (Smith and Wessel, 1990).

When the data constraints are noisy or too numerous to warrant an exact interpolation it is advantageous to solve the linear system (5) using the singular value decomposition method. We decompose $\mathbf{G} = \mathbf{USV}^T$ and find the coefficients

$$\mathbf{c} = \mathbf{G}^{-1}\mathbf{w} = \mathbf{VS}^{-1}\mathbf{U}^T\mathbf{w} \tag{32}$$

where $\mathbf{S}$ is a diagonal matrix of eigenvalues. By setting the inverse of the smallest eigenvalues to zero we improve the stability of the system at the expense of no longer interpolating the data exactly. The variance of the data explained

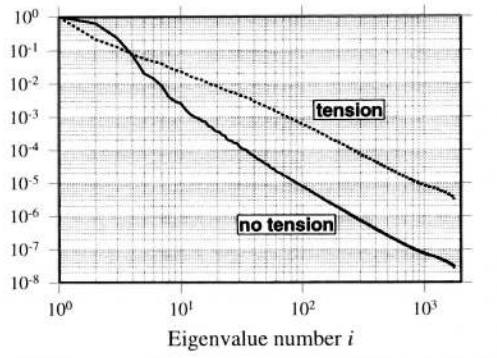

Figure 7. Comparison of decay in eigenvalues between solution in Figure 5 and complimentary solution without tension. Including tension gives each data point more influence away from point, resulting in less rapid decrease in eigenvalues. This fact makes spline in tension method more stable than minimum curvature method.

by the model is

$$\sigma_n^2 = \frac{1}{N}\sum_{i=1}^{N-n}\left[\sum_{j=1}^{N} u_{ji}w_j\right]^2 = f\frac{1}{N}\sum_{j=1}^{N} w_j^2 = f\sigma_0^2 \tag{33}$$

where n is the number of eigenvalues set to 0. For $n = 0$ we interpolate exactly, hence $f = 1$. If one wanted the surface only to explain 95% of the data variance (e.g., $f = 0.95$), then one could numerically solve (33) for n and only use the largest $N - n$ eigenvalues in (32).

The stability of the linear system is affected by the data distribution. As Sandwell (1987) reports, the system can become unstable when the ratio of the greatest point separation to the smallest point separation is large. However, by adding tension we greatly reduce the possibility of attempting to solve a near-singular system. This is perhaps best illustrated by inspecting the eigenvalues of the matrix **G** for situations with and without tension. Figure 7 shows the decay in eigenvalues for the minimum curvature case ($\tau = 0$; solid line) and the $\tau = 0.5$ case (dashed line) for the gridding of the multibeam bathymetry discussed previously (Fig. 5). As can be seen, the ratio of the eigenvalues to the largest eigenvalue λ_1 decays much slower with tension than without. For the smallest eigenvalues the ratios differ by almost 2 orders of magnitude. Thus, adding tension to the gridding greatly stabilizes the linear system and allows us to include more data than would be possible with the minimum curvature method, regardless of whether single or double precision is used.

The Projection Onto Convex Sets (POCS) method is versatile when the interpolating surface is required to satisfy several simultaneous criteria (Menke, 1991). One (of many) requirements may be that the power spectrum of the surface should follow a specified trend. POCS methods that implement power spectrum bounds can mimic a spline in tension by taking the Fourier transform of the surface and modifying the amplitude spectrum so that it does not exceed

$$s^2(\mathbf{k}) = A[|\mathbf{k}|^4 + p^2|\mathbf{k}|^2]^{-2} \quad (34)$$

at any wavenumber $\mathbf{k}$. The constant A is selected to equal the variance of the data. For values of $\mathbf{k}$ where the amplitude spectrum exceeds $s^2(\mathbf{k})$ the amplitude is reset to $s^2(\mathbf{k})$, leaving the phase spectrum unchanged.

Finally, one of the most rewarding aspects of the Green's function approach for splines in tension lies in the great simplification of the computer implementation of the method. For example, the Matlab script that solves the 2-D gridding using data constraints (and optional slope constraints) has one order of magnitude fewer source-code lines than the corresponding C program using finite differences (Smith and Wessel, 1990; Wessel and Smith, 1995); the bulk of these savings stems from the simple "bookkeeping" needed to solve the problem. Thus, our technique can be incorporated easily into task-specific functions with minimum development time regardless of computer language used.

ACKNOWLEDGMENTS

Terri Duennebier kindly provided the data used in Figure 5. This work was supported by the National Science Foundation under grant EAR-9303402. School of Ocean and Earth Science and Technology contribution number 4525.

REFERENCES

Abramowitz, M., and Stegun, I., eds., 1970, Handbook of mathematical functions: Dover, New York, 1046 p.

Bracewell, R. N., 1978, The Fourier transform and its applications (2nd ed.): McGraw-Hill Book Co., London, 444 p.

Briggs, I. C., 1974, Machine contouring using minimum curvature: Geophysics, v. 39, no. 1, p. 39–48.

Clark, I., 1979, Practical geostatistics: Applied Science Publ., London, 129 p.

Cline, A., 1974, Scalar and planar-value curve fitting using splines under tension: Comm. ACM., v. 17, p. 218–223.

Davis, J. C., 1986, Statistics and data analysis in geology (2 ed.): John Wiley & Sons, New York, 646 p.

Greenberg, M. D., 1971, Application of Green's functions in science and engineering: Prentice-Hall, Englewood Cliffs, New Jersey, 141 p.

Hardy, R. L., 1971, Multiquadric equations of topography an otehr irregular surfaces: Jour. Geophys. Res., v. 76, no. 8, p. 1905–1915.

Hardy, R. L., and Nelson, S. A., 1986, A multiquadric-biharmonic representation and approximation of the disturbing potential: Geophys. Res. Lett., v. 13, no. 1, p. 18–21.

Inoue, H., 1986, A least-squares smooth fitting for irregularly spaced data: Finite-element approach using the cubic B-spline basis: Geophysics, v. 51, no. 11, p. 2051–2066.

Menke, W., 1991, Applications of the POCS inversion method to interpolating topography and other geophysical fields: Geophys. Res. Lett., v. 18, no. 3, p. 435–438.

Mitásová, H., and Mitás, L., 1993, Interpolation by regularized spline with tension: I. Theory and implementation: Math. Geology, v. 25, no. 6, p. 641–655.

Olea, R. A., 1974, Optimal contour mapping using universal kriging: Jour. Geophys. Res. v. 79, no. 5, p. 696–702.

Sandwell, D. T., 1987, Biharmonic spline interpolation of Geos-3 and Seasat altimeter data: Geophys. Res. Lett., v. 14, no. 2, p. 139–142.

Schweikert, D. G., 1966, An interpolating curve using a spline in tension: Jour. Math. Physics, v. 45, p. 312–317.

Smith, W. H. F., and Wessel, P., 1990, Gridding with continuous curvature splines in tension: Geophysics, v. 55, no. 3, p. 293–305.

Swain, C. J., 1976, A FORTRAN IV program for interpolating irregularly spaced data using the difference equations for minimum curvature: Computers & Geosciences, v. 1, no. 4, p. 231–240.

Timoshenko, S., and Woinowsky-Krieger, S., 1959, Theory of plates and shells (2nd ed.): McGraw-Hill Book Co., New York, 580 p.

Wegman, E. J., and Wright, I. W., 1983, Splines in statistics: Jour. Am. Stat. Assoc., v. 78, no. 382, p. 351–365.

Wessel, P., and Smith, W. H. F., 1991, Free software helps map and display data: EOS Trans. AGU, v. 72, no. 41, p. 441, 445–446.

Wessel, P., and Smith, W. H. F., 1995, New version of the generic mapping tools released: EOS Trans. AGU, v. 76, no. 33, p. 329.

Wessel, P., and Smith, W. H. F., 1996, A global, self-consistent, hierarchical, high-resolution shoreline database: Jour. Geophys. Res., v. 101, no. B4, p. 8741–8743.